Crystal structure and lattice dynamics of AlB$_2$ under pressure and implications for MgB$_2$

I. Loa,[*] K. Kunc,[†] and K. Syassen

Max-Planck-Institut für Festkörperforschung, Heisenbergstrasse 1, D-70569 Stuttgart, Germany

P. Bouvier

European Synchrotron Radiation Facility, BP 220, F-38043 Grenoble, France

The effect of high pressures, up to 40 GPa, on the crystal structure and lattice dynamics of AlB$_2$ was studied by synchrotron x-ray powder diffraction, Raman spectroscopy, and first-principles calculations. There are no indications for a pressure-induced structural phase transition. The Raman spectra of the metallic sample exhibit a well-defined peak near 980 cm^{-1} at 0 GPa, which can be attributed to the Raman-active E_{2g} zone-center phonon. Al deficiency of $\sim 11\%$ in AlB$_2$, as indicated by the x-ray data, changes qualitatively the electronic structure, and there are indications that it may have a sizable effect on the pressure dependence of the E_{2g} phonon frequency. Similar changes of the pressure dependence of phonon frequencies, caused by nonstoichiometry, are proposed as an explanation for the unusually large variation of the pressure dependence of T_c for different samples of MgB$_2$.

I. INTRODUCTION

The AlB$_2$ structure type and derivatives thereof are among the most frequently occurring ones for intermetallic binary and ternary compounds.[1,2] Transition-metal diborides, belonging to this family, have been studied in some detail because of their potential application in electronic devices[3] to overcome current problems of electromigration, corrosion, and diffusion into the semiconductor substrate. The largest interest, however, has been undoubtedly received by the recently discovered superconductor MgB$_2$ that also crystallizes in the simple AlB$_2$ structure as depicted in Fig. 1.

AlB$_2$-type compounds have not been studied systematically at high pressures. There seem to exist no confirmed reports on pressure-induced structural phase transitions in metal diborides. There are, however, structural studies of the rare-earth metal digallides GdGa$_2$, HoGa$_2$, ErGa$_2$, and TmGa$_2$ at high pressures.[4–7] With the lighter rare-earth elements La—Er, the digallides crystallize in the AlB$_2$ structure at ambient pressure. In essence, all of the rare-earth metal digallides studied so far show a transition to the UHg$_2$ structure that is isotypic to AlB$_2$ but with a lower c/a ratio.

The superconductor MgB$_2$ was studied at high pressures with regard to its superconducting transition temperature,[8–13] crystal structure,[14–18] and lattice dynamics.[17,19] The pressure dependence of T_c could be well explained in the framework of phonon-mediated, i.e., BCS, superconductivity.[14,20,21] An isostructural transition near 30 GPa was reported[22] but could not be reproduced in another study up to 40 GPa.[18] Much higher pressures may be necessary to induce transitions possibly towards the UHg$_2$ structure.

We study here the effect of hydrostatic pressure on the crystal structure and lattice dynamics of AlB$_2$. Synchrotron x-ray powder diffraction and Raman-scattering experiments are complemented by first-principles calculations. The present high-pressure study was in part motivated by the question whether some of the unusual physical properties of MgB$_2$—such as the sizable anharmonicity[19,23,24] or the re-

markably large calculated pressure dependence[19] of the E_{2g} phonon—are specific to MgB$_2$ or whether they are characteristic of other AlB$_2$-type metal diborides as well. It aims at providing high-pressure structural and lattice dynamical information for comparison with corresponding data on MgB$_2$. Finally, Al deficiency appears to be hardly avoidable in the growth of AlB$_2$.[25,26] We show that it has significant effect on the electronic structure of AlB$_2$ and may also influence its lattice dynamics. We will discuss possible consequences of metal deficiency for the superconductor MgB$_2$ where this issue is also of relevance.

II. EXPERIMENTS

A. Experimental details

The structural properties of AlB$_2$ under pressure were studied up to 40 GPa by monochromatic ($\lambda = 0.3738$ Å) x-ray powder diffraction at the European Synchrotron Radiation Facility (ESRF Grenoble, beam line ID30). Commercially available AlB$_2$ powder (Alfa Aesar, 99%) was placed in a diamond-anvil cell (DAC) for pressure generation. Ni-
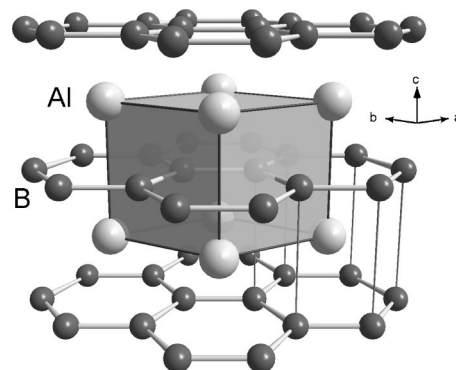

FIG. 1. Crystal structure of AlB$_2$. The boron atoms form honeycomb layers. Al atoms are located at the centers of hexagonal prisms that are formed by the B sheets.
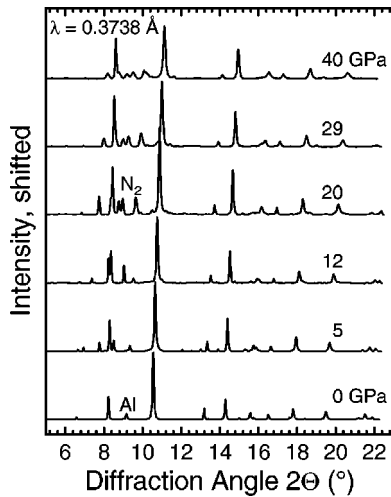
FIG. 2. X-ray powder diffraction diagrams of AlB_2 at various pressures ($T = 298$ K). "Al" marks a peak due to fcc-Al. Additional peaks appear at pressures above 2 GPa due to various phases of solid nitrogen.
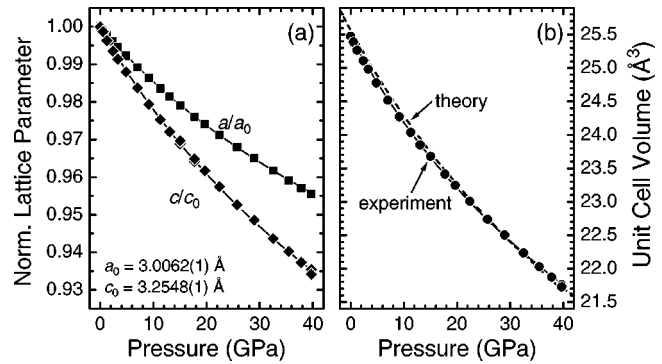

FIG. 3. (a) Experimental lattice parameters of AlB_2 as a function of pressure, normalized to their respective zero-pressure values. (b) Experimental (symbols and solid line) and calculated (dashed line) pressure-volume relations. The lines are given by the Murnaghan equation of state with the parameters listed in Table I.

trogen was employed as a pressure medium to provide nearly hydrostatic conditions. Diffraction patterns were recorded on image plates and then integrated[27] to yield intensity vs 2θ diagrams.

Raman spectra of AlB_2 up to 25 GPa (DAC, 4:1 methanol/ethanol mixture as a pressure medium) were excited at 633 nm utilizing a long-distance microscope objective. They were recorded in backscattering geometry using a single-grating spectrometer with a multichannel charge-coupled device (CCD) detector and a holographic notch filter for suppression of the laser line (Dilor Labram). For the Raman experiments, the DAC was equipped with synthetic diamonds (Sumitomo type IIa) which emit only minimal luminescence. In all experiments, pressures were measured with the ruby luminescence method.[28]

B. X-ray diffraction under pressure

Figure 2 shows x-ray-diffraction patterns of AlB_2 for increasing pressures up to 40 GPa. The diagrams evidence small amounts of Al metal as a secondary phase. At pressures above 2 GPa, additional reflections are observed due to various phases of solid nitrogen. There are no indications for a pressure-induced structural phase transition in AlB_2 up to 40 GPa.

The lattice parameters as a function of pressure were determined from Rietveld-type fits of the diffraction diagrams. The compressibility of AlB_2 is moderately anisotropic as illustrated in Fig. 3(a) with the softer direction being parallel to the c axis. Up to 40 GPa, compression along c is 47% larger than along a. The c/a ratio decreases from 1.083 (0 GPa) to 1.060 at 40 GPa. From the lattice parameters, we determine the unit-cell volume as a function of pressure as shown in Fig. 3(b). The data are well represented by the Murnaghan relation[29] $V(P) = V_0[(B'/B_0)P + 1]^{-1/B'}$. With $V_0 = 25.4734(5)$ Å^3 fixed at the value determined from the zero-pressure data, we obtain by least-squares fitting the bulk modulus B_0 and its pressure derivative B' at zero pressure as listed in Table I.

Rietveld refinements of the crystal structure with the Al site occupation as a free parameter indicate that the sample studied here has an Al deficiency of $\sim 11\%$. This is illustrated in Fig. 4 where the difference curves for refinements of $Al_{1.00}B_2$ and $Al_{0.89}B_2$ are shown together with the experimental diffraction pattern. A Stephens peak profile[30] was used and a common isotropic thermal parameter for Al and B was optimized. The weighted profile R value (without background) reduces from $R_{wp} = 8.5\%$ for $Al_{1.00}B_2$ to $R_{wp} = 6.9\%$ for $Al_{0.89}B_2$. This indication of substantial Al deficiency in AlB_2 is in agreement with previous chemical analysis data,[25] density measurements,[25,26] and recent single-crystal x-ray-diffraction results.[26]

TABLE I. Structural parameters of AlB_2 and MgB_2: zero-pressure volume V_0 and lattice constants a_0, c_0; bulk modulus B_0, and its pressure derivative B' at zero pressure. Variation of the c/a ratio with pressure is described by the quadratic polynomial $c/a = c_0/a_0 + \alpha P + \beta P^2$, with the coefficients α, β as listed below.

	V_0 (Å^3)	a_0 (Å)	c_0 (Å)	B_0 (GPa)	B'	c_0/a_0	α (GPa^{-1})	β (GPa^{-2})
AlB_2, Expt. (300 K)	25.473(1)	3.0062(1)	3.2548(1)	170(1)	4.8(1)	1.0827(1)	$-8.8(1) \times 10^{-4}$	$0.77(4) \times 10^{-5}$
AlB_2, Calculated (DFT/GGA)	25.565	2.9977	3.2855	176.8	3.64	1.096	-12.0×10^{-4}	1.09×10^{-5}
MgB_2, Expt. (300 K)[b]	28.99(1)	3.0834(3)	3.5213(6)	147–155[a]	(4.0)[a]			

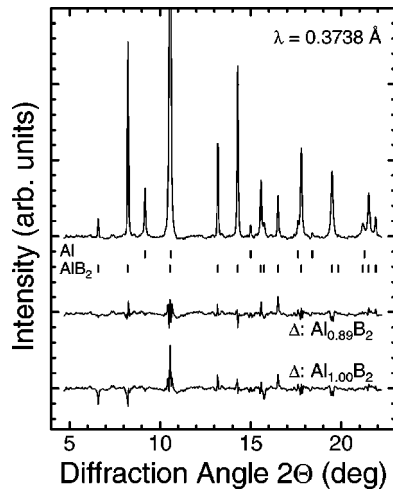[a]References 14, 16, and 17 with the assumption that $B' = 4$.
[b]Reference 72.

FIG. 4. X-ray powder diffraction diagram of AlB_2 at 0 GPa and 293 K, and difference curves ($\Delta = I_{expt.} - I_{calc}$) for refinements with and without Al deficiency. Markers show peak positions due to AlB_2 and fcc-Al.

C. Raman spectra at ambient conditions

AlB_2 has one Raman-active zone-center phonon mode.[31] It is an in-plane vibration of the B atoms with E_{2g} symmetry, where neighboring B atoms move out of phase.[19] The powder sample we investigated contained some small shiny crystallites up to ~ 10 μm in size. Figure 5 shows Raman spectra recorded on two different crystallites and at a sample spot where no crystallites were discernible with an optical microscope. Besides a Lorentzian-shaped peak [FWHM (full width at half maximum) of 40–50 cm^{-1}] which was attributed to the E_{2g} mode previously,[31] we observe an additional steplike feature at the lower-energy side of the main peak. It is clearly visible in the single-crystal spectra and reduces to a weak shoulder in the powder spectrum. The powder spectrum resembles that reported by Bohnen *et al.*[31] The peak position of the E_{2g} mode of the two crystallites differs by
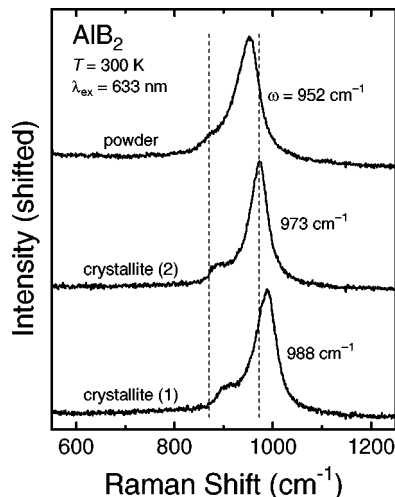

FIG. 5. Raman spectra of AlB_2 at ambient conditions recorded on two crystallites and at a sample spot where no crystallites were discernible ("powder").
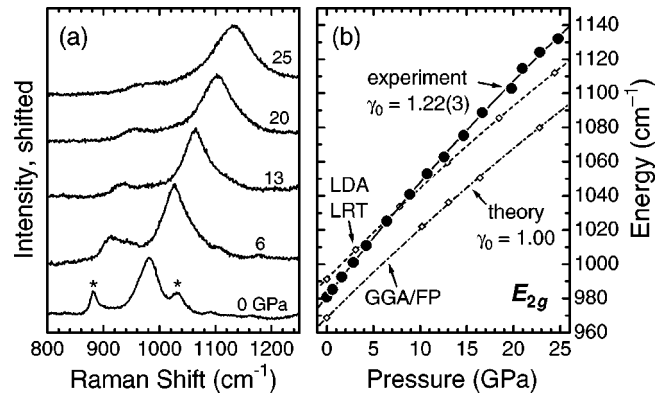

FIG. 6. (a) Raman spectra of AlB_2 recorded for increasing pressures of 0–25 GPa ($T = 300$ K). Peaks marked by asterisks are due to the methanol/ethanol pressure medium. (b) Experimental and calculated energies of the E_{2g} phonon mode. Experimental data are represented by circles and a solid line, results of the GGA/frozen-phonon and LDA/linear-response-theory calculations by a dash-dotted and dashed line, respectively. The lines represent quadratic functions fitted to the data.

15 cm^{-1} ($\omega = 973$ and 988 cm^{-1}). In the powder spectrum, the main peak occurs at an even lower energy of 952 cm^{-1}. The steplike feature in the spectra of the crystallites shifts by the same amount as the main peak, indicating that it is intrinsic to AlB_2. It appears likely that it is related to a peak in the calculated phonon density of states,[31] which exists slightly below the energy of the E_{2g} mode.

D. Raman spectra under pressure

Raman spectra of AlB_2 were recorded for increasing pressures up to 25 GPa. Since the sample is somewhat deformed when pressure is applied and there seems to be some inhomogeneity of the powder, several spectra were collected at different locations of the sample. The spectra shown in Fig. 6(a) result from averaging about five spectra recorded at different spots that were selected for a narrow E_{2g} peak and low background. The zero-pressure frequency of the E_{2g} mode in these averaged diagrams amounts to 981(1) cm^{-1}. Two additional peaks near 875 and 1025 cm^{-1} (at 0 GPa) are due to the methanol/ethanol pressure medium.

The E_{2g} phonon frequency increases continuously with increasing pressure, but with slightly decreasing slope $d\omega/dP$. The zero-pressure mode-Grüneisen parameter amounts to $\gamma_0 = 1.22(3)$ [based on $B_0 = 170(1)$ GPa]. Up to 10 GPa the peak width (FWHM) is essentially constant at 44 ± 2 cm^{-1}, while at higher pressures it increases to ~ 90 cm^{-1} at 25 GPa. This is most likely related to the solidification of the pressure medium near 10 GPa. From the Raman data there are no indications for a structural phase transition.

III. CALCULATIONS

A. Theoretical method

The theoretical methods employed here were described in detail in the context of our recent work on MgB_2.[19] In sum-

TABLE II. Pressure and volume dependences of selected phonon frequencies of AlB_2 and MgB_2. The zero-pressure frequency ω_0 and the linear and quadratic pressure coefficients were obtained by least-squares fits of $\omega(P) = \omega_0 + \alpha P + \beta P^2$ to the data. The theoretical mode-Grüneisen parameters γ_0 (at the theoretical equilibrium volume) are derived from a similar quadratic expression for $\omega(V)$. P has been obtained from V through the calculated P-V relation (see text). The experimental mode-Grüneisen parameter is determined from $\omega(P)$ and the experimental P-V relation.

Compound	Mode	ω_0 (cm^{-1})	α (cm^{-1}/GPa)	β (cm^{-1}/GPa^2)	γ_0
AlB_2	E_{2g}	969	5.425	-0.0235	1.00
	E_{2g} (Expt.)	981(1)	7.027	-0.0365	1.22(3)
	B_{1g}	490	2.968	-0.0087	1.06
MgB_2	E_{2g}	535	8.974	-0.0780	2.5
	B_{1g}	695	3.065	-0.0190	0.6

mary, first-principles calculations of the total energy E_{tot} of the solid are the basis for the determination of the equation of state and of the phonon frequencies. The energy is computed within the density-functional theory (DFT) using a plane-wave basis and pseudopotentials.

For part of the actual calculations (equation of state and phonon frequencies in the *frozen-phonon approach*), we employed the VASP codes[32–35] within the generalized gradient approximation (GGA).[36] The ultrasoft Vanderbilt-type pseudopotentials[37] were supplied by Kresse and Hafner.[38] The pseudopotential for Al treats explicitly three valence electrons $(3s^2 3p)$; no semicore states are included. A ''harder'' variant of the potential was chosen and the nonlinear core correction[39] is applied in order to improve the transferability. The calculations are carried out with a plane-wave cutoff energy of 23.6 Ry, and the Brillouin-zone sampling is based on a Γ centered $16 \times 16 \times 16$ uniform mesh, yielding 270 to 1170 k points in the irreducible wedge of the Brillouin zone, depending on the symmetry of the lattice [equilibrium structure or crystal with the displacements of the $E_{2g}(\Gamma)$ phonon]. As the system is metallic, the k-space integration with the incompletely filled orbitals uses the tetrahedron method[40] with Blöchl's corrections.[41]

The phonon frequencies were independently verified using the linear-response theory[42,43] as implemented in the ABINIT package[44] within the local-density approximation (LDA)[48,49] to the DFT. We used Hartwigsen-Goedecker-Hutter pseudopotentials,[50] treating $Al(3s^2 3p)$ and $B(2s^2 2p)$ levels as valence states, a plane-wave cutoff of 60 Ry, and a $12 \times 12 \times 12$ k-point mesh. A Gaussian smearing with a broadening parameter of 0.04 Ry was applied to improve k-point sampling in the special points method. The structural parameters were optimized for each volume/pressure such that the stress tensor components σ_{xx} and σ_{zz} agreed within 10^{-3} GPa.

B. Structural properties

For fourteen unit-cell volumes in the range 21.8–26.2 Å^3, we calculated (with the VASP codes) the total energy $E(V)$ for different c/a values, thus determining the optimized

structures $[a(V), c(V)]$ and minimized total energies. The latter data were fitted by the Murnaghan relation for $E(V)$ (Ref. 29)

$$E(V) = E_0 + \frac{B_0 V_0}{B'}\left[\frac{V}{V_0} + \frac{(V/V_0)^{1-B'} - B'}{B' - 1}\right], \quad (1)$$

which provided the static equilibrium volume V_0 as well as the bulk modulus B_0 and its pressure derivative B' at zero pressure. The structural parameters are summarized in Table I. The pressure-volume relation, shown in Fig. 3(b), compares well with the experimental data. The calculated equilibrium volume is 0.4% larger than the volume measured at 300 K. The individual lattice parameters are -0.3% off the experiment for a_0, $+0.9\%$ for c_0, and consequently $+1.2\%$ for c_0/a_0. The variation of c/a under pressure can be represented by a quadratic function and its coefficients are given in Table I.

C. Phonon frequencies

The energies of the E_{2g} phonon mode as a function of pressure were initially calculated in the frozen-phonon (FP) approach using the VASP codes and the GGA. For each phonon at a particular pressure value, the atoms are given six different displacements ranging from $u/a = 0.005$ to 0.035, and the calculated energy values $E(u)$ are fitted with a quartic polynomial. The resulting harmonic phonon frequencies and their respective pressure dependences are listed in Table II, together with the experimental data for the E_{2g} mode and our previous FP-GGA results for MgB_2[19]. As illustrated in Fig. 6(b), the calculated zero-pressure frequency is only $\sim 1\%$ lower than the experimental value, which is in the typical range for the difference between the experiment and the calculations of this type. Regarding the pressure dependence of the phonon frequency, however, we find an unusually large deviation of the theoretical results from the experiment. From the variation of the calculated phonon frequency with volume, we obtain a zero-pressure mode-Grüneisen parameter of $\gamma_0 = 1.00$ whereas the experimental value amounts to $\gamma_0 = 1.22(3)$.

Since the deviation of the theoretical results from the experimental data is larger than usual, we performed a second calculation of the E_{2g} frequency under pressure using a rather different approach, namely linear-response-theory (LRT) in the LDA with the ABINIT package. Consistent with the common overestimation of bond strengths in the LDA, we obtain here a somewhat larger zero-pressure phonon frequency, such that the two theoretical values bracket the experimental data at zero pressure. Over the whole pressure range the LDA/LRT calculation gives phonon frequencies that are consistently $\sim 2.4\%$ larger than the corresponding GGA/FP results. Consequently, we obtain essentially the same pressure dependence $d \ln \omega / dP$ for the two calculations. The deviation of the calculations from the experimental data is far beyond the typical uncertainty of such computations. The important difference between the theory and the experiment could be that the former is based on the ideal stoichiometry Al_1B_2, whereas the real sample is Al deficient.

For comparison with previous calculations for MgB_2, we have also calculated the frequency ω of the B_{1g} phonon in AlB_2 (out-plane motion of the boron atoms[19]), see Table II. The pressure dependence is characterized by a mode-Grüneisen parameter $\gamma_0 = 1.06$. In case of a constant, i.e., pressure independent $\gamma(V) \equiv \gamma_0$, the relation $\omega(V) = \omega_0 (V/V_0)^{-\gamma_0}$ holds. Thus, for both the E_{2g} and the B_{1g} mode in AlB_2, with $\gamma \approx 1$, there is a nearly inverse-proportional relation between the phonon frequency and volume. This is quite different from the situation in MgB_2 where we do not only have the very large $\gamma_0 = 2.5$ for the E_{2g} mode as noted before, but also a rather small $\gamma_0 = 0.6$ for the B_{1g} phonon (Table II).

The frozen-phonon calculations also yield information on the anharmonicity of the phonon modes as described in the context of our MgB_2 calculations.[19] In essence, the variation of the total energy with atomic displacement $E_{tot}(u)$ can be represented by a polynomial where the ratio of the quartic to squared quadratic coefficients a_4/a_2^2 is a measure of anharmonicity. In the harmonic limit, $a_4 = 0$. For the E_{2g} mode in AlB_2, we obtain $|a_4/a_2^2| < 0.01$ eV^{-1} which is about three orders of magnitude lower than the corresponding values for MgB_2 of $a_4/a_2^2 = 4-8$ eV^{-1} (see Refs. 19, 23). Small anharmonicities are calculated for the B_{1g} modes of both compounds: $a_4/a_2^2 = 0.27$ for AlB_2 and $a_4/a_2^2 = -0.05$ for MgB_2.

IV. DISCUSSION

A. Structural stability

In our x-ray-diffraction and Raman experiments, we do not find any indication for a structural phase transition or modulation of the structure. Group-subgroup symmetry considerations[2] indicate numerous possible distortions of the aristotype AlB_2 most of which are realized in intermetallic compounds at ambient pressure. The pressure-induced structural phase transitions of XY_2 intermetallic compounds have not been studied systematically. In the context of the AlB_2 structure a number of rare-earth metal digallides,[4–7] KHg_2,[51] and $LaCu_2$ (Ref. 52) were investigated at high pressures.

From the available data, a transition between the structure types AlB_2 and UHg_2 appears as a typical route. The KHg_2 ($CeCu_2$) structure type may occur as an intermediate phase. AlB_2 and UHg_2 are isopointal structures, distinguished only by their c/a ratios. Two clearly separated groups of compounds of AlB_2 and UHg_2 type are observed when plotting the c/a ratio versus the ratio of the metallic radii of XY_2 intermetallic compounds.[6,53,54] The AlB_2- and UHg_2-type branches are characterized by c/a ratios of 0.95–1.20 and 0.60–0.85, respectively. The compound AlB_2 with $c/a = 1.083$ (at 0 GPa) is located near the center of the former branch. In the pressure range, up to 40 GPa, explored here it decreases only to 1.060. Pressures well above 1 Mbar may therefore be needed for a possible transition towards the UHg_2 structure. At lower pressures, a transition involving a buckling of the boron honeycomb layers may occur, which could lead to phases of the $CeCu_2$, $CeCd_2$, or $CaIn_2$ type.[2,6]

B. Raman spectra of AlB_2 vs MgB_2

Raman spectroscopy is commonly applied to semiconductors and insulators, but only to a much smaller extend to metals. It is essentially the group of elemental hcp metals that has been studied systematically, already in the late 1960s at ambient pressure[55] and more recently at high pressures (see e.g., Refs. 56, 57 and references therein). It may therefore be attributed to the lack of reference data that the observation of a very broad Raman feature in MgB_2 near 600 cm^{-1} (FWHM of ~ 300 cm^{-1}) led to a still unresolved controversy over the origin of this peak. It has initially been attributed[31] to the Raman-active E_{2g} mode, which immediately raises the question of the large linewidth. The large peak width has been related to the strong electron-phonon coupling and to structural disorder. The latter now appears less likely because Raman spectra of MgB_2 powders are quite similar to those of recently available small single crystals[58,59] that are presumably less disordered. High-pressure Raman experiments[19] have cast doubt on the assignment to the E_{2g} phonon. They revealed a double-peak structure with peaks at 603(6) cm^{-1} and 750(20) cm^{-1}. Neither of the two peaks could be attributed to the E_{2g} mode because of severe deviations from the calculated phonon frequencies in terms of zero-pressure frequencies and/or the pressure dependences.

The present Raman data of AlB_2 show that it is possible to obtain Raman spectra with a well-defined E_{2g} peak from the metallic samples of the AlB_2 structure. The difficulties encountered in case of MgB_2 are therefore not likely related to the metallicity of the sample nor intrinsic to the structure type. Crystallinity also appears to have only a small effect on the Raman spectrum as the Raman linewidth of the AlB_2 powder sample is comparable to that of the AlB_2 crystallites.

There are two properties of MgB_2 with regard to phonons which make it distinct from AlB_2. First, the whole E_{2g} phonon branch along the Γ-A direction in the Brillouin zone exhibits very strong electron-phonon coupling in MgB_2.[23,60–62] Second, the $E_{2g}(\Gamma)$ mode shows pronounced anharmonicity.[19,23] Both electron-phonon and phonon-phonon interaction decrease the phonon lifetime and hence
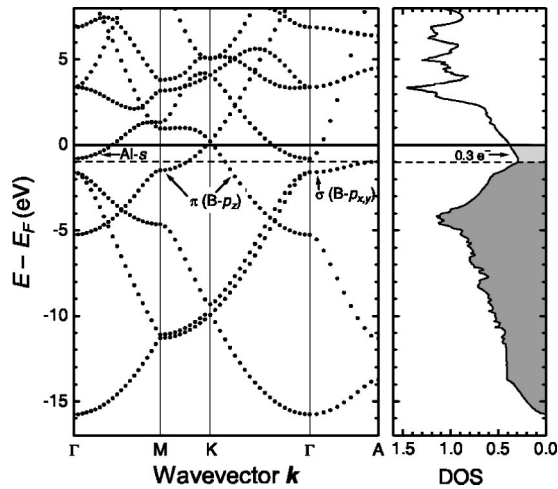
FIG. 7. Calculated electronic band structure and density of states (DOS) of AlB_2 at ambient pressure. Energies are given with respect to the Fermi energy E_F. The DOS is given in units of (states/eV)/formula unit.

increase the phonon linewidth.[63] They are therefore the most likely causes for the absence of a well-defined E_{2g} Raman peak in MgB_2.

C. Metal deficiency in AlB_2

Our x-ray-diffraction data indicate an Al deficiency of 11% in AlB_2 in accord with previous density measurements and chemical analysis,[25,26] as well as recent single-crystal x-ray-diffraction results.[26] Although the change of the E_{2g} phonon frequency at different sample spots suggests that there is some variation of the Al content, there is no indication that growth of aluminum diboride in the composition $Al_{1.0}B_2$ is possible. The occurrence of substantial metal deficiency appears to be common to many (transition) metal diborides.[64]

In case of AlB_2, this metal deficiency has important influence on the electronic structure. A comparison of the calculated band structures of AlB_2 and MgB_2 shows that the relative ordering and dispersions of the bands near the Fermi level are very similar. The difference between AlB_2 and MgB_2 can largely be treated in a rigid-band picture with a higher band filling for AlB_2. It is therefore justified to discuss the observed Al deficiency of $\sim 10\%$ in a rigid-band picture, too. Figure 7 shows the calculated electronic band structure[65] and density of states of AlB_2. In case of the stoichiometric compound the π-type bands derived from the boron p_z states and the bands with Al-s character (near Γ) are partially filled and give rise to the metallic state. 10% deficiency of Al removes 0.3 valence electrons and consequently lowers E_F by 0.9 eV, which leads to a *complete depletion of the band with* Al-s *character*. In other words, the experimentally observed Al deficiency is expected to lead to a qualitative change in the electronic structure compared to the ideal case of Al_1B_2. In terms of the Fermi surface this change means a removal of the electron pocket around Γ.

The measured mode-Grüneisen parameter of the $Al_{0.9}B_2$ sample is $\sim 20\%$ larger than calculated for $Al_{1.0}B_2$, a deviation that is far beyond the typical uncertainty of such computations. The zero-pressure phonon frequency, on the other hand, seems to be hardly affected. The apparent difference between experiment and calculation is the Al deficiency of the sample, which was not taken into account in the theory. We tentatively attribute the discrepancy between the experimental and calculated mode-Grüneisen parameters to the Al-deficiency-induced electronic changes discussed above. However, it cannot be excluded at this point that other effects are also at work. A more detailed analysis of the effect of Al deficiency on the electronic and lattice dynamical properties of AlB_2 is, however, beyond the scope of this work.

D. Metal deficiency in MgB_2

Mg deficiency in MgB_2 was often indicated by the occurrence of MgO as a secondary phase in MgB_2 samples that were grown from a molar 1:2 mixture of Mg and B. The variations of T_c and even more of the pressure dependence of T_c for different samples appeared to be related to nonstoichiometry of the material. The correlation between composition, structural parameters and T_c has been established in an experiment by Indenbom *et al.*[69] By diffusion of Mg into a boron cylinder they produced a sample with a composition changing gradually between $Mg_{1.0}B_2$ and $Mg_{0.8}B_2$. With decreasing Mg content, the lattice parameter c is increased by 0.003 (0.1%) and T_c is increased from 37.2 to 39.0 K.

Tissen *et al.*[12] furthermore pointed out a correlation between the zero-pressure critical temperature $T_{c,0}$ and the pressure derivative dT_c/dP: As $T_{c,0}$ increases from 37.3 to 39.2 K, for various samples, dT_c/dP changes from -2.0 to -1.1 K/GPa. Monteverde *et al.*[9] discussed a similar observation on a smaller number of samples in terms of the electronic band structure and band-filling effects related to the Mg nonstoichiometry. On the other hand, the pressure-induced changes of the electronic density of states calculated for MgB_2 are too small to account for the observed decrease of T_c under compression.[20] It is rather the increase in the relevant phonon frequencies which provides the main contribution to the pressure dependence of T_c.[14,20,21] It would therefore be rather surprising if electronic density effects— i.e., the electronic density $N(E_F)$ at the Fermi level—were responsible for the large sensitivity of dT_c/dP on Mg non-stoichiometry.

The indications that Al deficiency in AlB_2 may affect the pressure dependence of the E_{2g} phonon frequency hints at an alternative possible explanation for the large sensitivity of dT_c/dP on Mg deficiency in MgB_2. It was first pointed out by Yildirim *et al.*[23] that the E_{2g} phonon mode in MgB_2 exhibits a very large anharmonicity. Boeri *et al.*[70] showed theoretically that this effect arises in MgB_2 because here the Fermi level E_F is located only ~ 0.5 eV below the top of σ bands of the equilibrium structure. The lattice distortion of the E_{2g} mode induces a splitting of these σ bands large enough that the lower split-off band sinks completely below E_F.[61,70] This does not happen in AlB_2 and graphite, and anharmonicity is indeed negligible.

It is also noteworthy that the E_{2g} mode in AlB_2 is much higher in energy than the B_{1g} phonon, whereas the reversed

order is calculated for MgB_2 (see Table II) although both compounds are structurally quite similar. This effect was pointed out before and studied in $Mg_{1-x}Al_xB_2$ mixed crystals by Renker et al.[71] The interchange, which occurs only in undoped or moderately substituted material ($0 < x < 0.2$), was also attributed to the electronic changes, especially the disappearance of the hole pockets from the Fermi surface for $x > 0.2$.

The metal content in MgB_2 affects the band filling, a larger Mg deficiency moving the Fermi level further below the top of the σ bands. It is therefore to be expected that the anharmonicity of the E_{2g} mode should decrease with decreasing Mg content. Lattice dynamical calculations showed that the E_{2g} anharmonicity decreases with increasing pressure[19] and the initially very large mode-Grüneisen parameter decreases too.[19] If the mode-Grüneisen parameters decreases as function of band filling at ambient pressure, i.e., due to nonstoichiometry of MgB_2, it would, qualitatively, lead to the observed relation between dT_c/dP and Mg deficiency. This effect would be a manifestation of the changes of the lattice dynamics rather than changes of the electronic density of states. A more detailed and quantitative analysis is certainly needed, but the present results are indication of the importance of stoichiometry with regard to the superconducting properties of MgB_2, specifically the pressure dependence of T_c.

V. CONCLUSIONS

We have studied the crystal structure of AlB_2 by x-ray powder diffraction up to 40 GPa. The compressibility is moderately anisotropic, consistent with the anisotropic bonding properties. In the pressure range studied here, we did not observe a structural phase transition. Our x-ray-diffraction data indicate an Al deficiency of $\sim 11\%$ in agreement with previous reports. Despite the neglect of this nonstoichiometry in our first-principles calculations, the calculated structural properties are in good agreement with the experiment.

The E_{2g} zone-center phonon in metallic AlB_2 can be observed as a well-defined Raman peak. We conclude that the lack of such a Raman feature in MgB_2 is neither related to the metallicity or disorder of the sample nor is it a generic property of AlB_2-type compounds. Our observations rather support the view that it is due to the strong electron-phonon coupling and/or anharmonicity, which are distinct properties of MgB_2. We found some deviation of the calculated pressure dependence of the E_{2g} phonon frequency of AlB_2 from the experimental data and tentatively attributed this to the Al deficiency of the AlB_2 sample, which was not taken into account in the theory.

The correlations between nonstoichiometry of MgB_2 and its superconducting properties have been pointed out previously. Here we considered the possible effects of Mg deficiency in MgB_2 on its electronic structure and lattice dynamics. The anticipated changes are consistent with the available experimental data on the correlation between Mg content and the pressure dependence of T_c. This leads us to propose that the large variation of the pressure dependence of T_c (-0.7 to -2.0 K/GPa) in MgB_2 in various experiments may be caused by the effect of nonstoichiometry on the lattice dynamics, mediated via changes in the electronic structure of MgB_2.

*Electronic address: I.Loa@fkf.mpg.de

†Permanent address: CNRS and Université P. et M. Curie, Laboratoire d'Optique des Solides UMR7601, T13-C80, 4 pl. Jussieu, 75252 Paris, Cédex 05, France.

[1] P. Villars and L.D. Calvert, *Pearsons's Handbook of Crystallographic Data for Intermetallic Phases*, 2nd ed. (American Society for Metals, Materials Park, OH, 1991).

[2] R.-D. Hoffman and R. Pöttgen, Z. Kristallogr. **216**, 127 (2001).

[3] W.S. Williams, JOM **49**, 38 (1997).

[4] U. Schwarz, S. Bräuninger, U. Burkhardt, K. Syassen, and M. Hanfland, Z. Kristallogr. **216**, 331 (2001).

[5] U. Schwarz, S. Bräuninger, Y. Grin, K. Syassen, and M. Hanfland, J. Alloys Compd. **268**, 161 (1998).

[6] S. Bräuninger, U. Schwarz, and K. Syassen (unpublished).

[7] U. Schwarz, S. Bräuninger, Y. Grin, and K. Syassen, J. Alloys Compd. **245**, 23 (1996); **256**, 279 (1997).

[8] A. Saito, T. Taknenobu, T. Ito, Y. Iwasa, K. Prassides, and T. Arima, J. Phys.: Condens. Matter **13**, L267 (2001).

[9] M. Monteverde, M. Núñez-Regueiro, N. Rogado, K.A. Regan, M.A. Hayward, T. He, S.L. Loureiro, and R.J. Cava, Science **292**, 75 (2001).

[10] B. Lorenz, R.L. Meng, and C.W. Chu, Phys. Rev. B **64**, 012507 (2001).

[11] T. Tomita, J.J. Hamlin, J.S. Schilling, D.G. Hinks, and J.D. Jorgensen, Phys. Rev. B **64**, 092505 (2001).

[12] V.G. Tissen, M.V. Nefedova, N.N. Kolesnikov, and M.P. Kulakov, Physica C **363**, 194 (2001).

[13] B. Lorenz, R.L. Meng, and C.W. Chu, cond-mat/0104303 (unpublished).

[14] T. Vogt, G. Schneider, J. Hriljac, G. Yang, and J. Abell, Phys. Rev. B **63**, 220505 (2001).

[15] K. Prassides, Y. Iwasa, T. Ito, D.H. Chi, K. Uehara, E. Nishibori, M. Takata, M. Sakata, Y. Ohishi, O. Shimomura, T. Muranaka, and J. Akimitsu, Phys. Rev. B **64**, 012509 (2001).

[16] J.D. Jorgensen, D.G. Hinks, and S. Short, Phys. Rev. B **63**, 224522 (2001).

[17] A.F. Goncharov, V.V. Struzhkin, E. Gregoryanz, J. Hu, R.J. Hemley, H. Mao, G. Lapertot, S.L. Bud'ko, and P.C. Canfield, Phys. Rev. B **64**, 100509 (2001).

[18] P. Bordet, M. Mezouar, M. Núñez-Regueiro, M. Monteverde, M.D. Núñez-Regueiro, N. Rogado, K.A. Regan, M.A. Hayward, T. He, S.M. Loureiro, and R.J. Cava, Phys. Rev. B **64**, 172502 (2001).

[19] K. Kunc, I. Loa, K. Syassen, R.K. Kremer, and K. Ahn, J. Phys.: Condens. Matter **13**, 9945 (2001).

[20] I. Loa and K. Syassen, Solid State Commun. **118**, 279 (2001).

[21] X.J. Chen, H. Zhang, and H.-U. Habermeier, Phys. Rev. B **65**, 144514 (2002).

[22] S. Li-Ling, T. Kikegawa, W. Qi, Z. Zai-Ji, and W. Wen-Kui, Chin. Phys. Lett. **18**, 1401 (2001).

[23] T. Yildirim, O. Gülseren, J.W. Lynn, C.M. Brown, T.J. Udovic, H.Z. Qing, N. Rogado, K. Regan, M. Hayward, J. Slusky, T. He, M. Haas, P. Khalifah, K. Inumaru, and R. Cava, Phys. Rev. Lett. **87**, 037001 (2001).

[24] A.Y. Liu, I.I. Mazin, and J. Kortus, Phys. Rev. Lett. **87**, 087005 (2001).

[25] V.I. Matkovich, J. Economy, and R.F. Giese, Jr., J. Am. Chem. Soc. **84**, 2337 (1964).

[26] U. Burkhardt, V. Gurin, W. Schnelle, H. Borrmann, and Y. Grin, Max-Planck-Institut für Chemische Physik fester Stoffe, Dreseen, Germany, Annual Report 2000.

[27] A. Hammersley, computer code FIT2D (ESRF, Grenoble, 1998).

[28] H.K. Mao, J. Xu, and P.M. Bell, J. Geophys. Res. **91**, 4673 (1986).

[29] F.D. Murnaghan, Proc. Natl. Acad. Sci. U.S.A. **30**, 244 (1944).

[30] P.W. Stephens, J. Appl. Crystallogr. **32**, 281 (1999).

[31] K.-P. Bohnen, R. Heid, and B. Renker, Phys. Rev. Lett. **86**, 5771 (2001).

[32] G. Kresse and J. Hafner, Phys. Rev. B **47**, R558 (1993).

[33] G. Kresse, Ph.D. thesis, Technische Universität Wien, 1993.

[34] G. Kresse and J. Furthmüller, Comput. Mater. Sci. **6**, 15 (1996).

[35] G. Kresse and J. Furthmüller, Phys. Rev. B **54**, 11 169 (1996).

[36] J.P. Perdew and Y. Wang, Phys. Rev. B **45**, 13 244 (1992).

[37] D. Vanderbilt, Phys. Rev. B **41**, 7892 (1990).

[38] G. Kresse and J. Hafner, J. Phys.: Condens. Matter **6**, 8245 (1994).

[39] S.G. Louie, S. Froyen, and M.L. Cohen, Phys. Rev. B **26**, 1738 (1982).

[40] O. Jepsen and O.K. Andersen, Solid State Commun. **9**, 1763 (1971).

[41] P.E. Blöchl, O. Jepsen, and O.K. Andersen, Phys. Rev. B **49**, 16 223 (1994).

[42] X. Gonze, Phys. Rev. B **55**, 10 337 (1997).

[43] X. Gonze and C. Lee, Phys. Rev. B **55**, 10 355 (1997).

[44] The ABINIT code is a common project of the Université Catholique de Louvain, Corning Incorporated, and other contributors (URL http://www.abinit.org). It relies on an efficient Fast Fourier Transform algorithm (Ref. 45) for the conversion of wave functions between real and reciprocal space, on the adaptation to a fixed potential of the band-by-band conjugate-gradient method (Ref. 46) and on a potential-based conjugate-gradient algorithm for the determination of the self-consistent potential (Ref. 47).

[45] S. Goedecker, SIAM J. Sci. Comput. (USA) **18**, 1605 (1997).

[46] M. Payne, M. Teter, D. Allan, T. Arias, and J. Joannopoulos, Rev. Mod. Phys. **64**, 1045 (1992).

[47] X. Gonze, Phys. Rev. B **54**, 4383 (1996).

[48] J.C. Slater, Phys. Rev. **81**, 385 (1951).

[49] W. Kohn and L.J. Sham, Phys. Rev. **140**, A1133 (1965).

[50] C. Hartwigsen, S. Goedecker, and J. Hutter, Phys. Rev. B **58**, 3641 (1998).

[51] H.-J. Beister, K. Syassen, H.-J. Deiseroth, and D. Toelstede, Z. Naturforsch. B **48b**, 11 (1993).

[52] A. Lindbaum, S. Heathman, G. Kresse, M. Rotter, E. Gratz, A. Schneidewind, G. Behr, K. Litfin, T. Le Bihan, and P. Svoboda, J. Phys.: Condens. Matter **12**, 3219 (2000).

[53] W. B. Pearson, *The Crystal Chemistry and Physics of Metals and Alloys* (Wiley Intersciences, New York, 1972).

[54] W.B. Pearson, Proc. R. Soc. London, Ser. A **365**, 523 (1979).

[55] J. H. Parker, Jr., D. W. Feldman, and M. Ashkin, in *Light Scattering Spectra of Solids*, edited by G. B. Wright (Springer-Verlag, New York, 1969), pp. 389–397.

[56] H. Olijnyk, A.P. Jephcoat, and K. Refson, Europhys. Lett. **53**, 504 (2001).

[57] H. Olijnyk and A. Jephcoat, Solid State Commun. **115**, 335 (2000).

[58] J. Hlinka, I. Gregora, J. Pokorný, A. Plecenik, P. Kúš, L. Satrapinsky, and Š. Beňačka, Phys. Rev. B **64**, 140503 (2001).

[59] H. Martinho, A.A. Martin, C. Rettori, O.F. de Lima, R.A. Ribeiro, M.A. Avila, P.G. Pagliuso, N.O. Moreno, and J.L. Sarrao, cond-mat/0105204v4 (unpublished).

[60] J. Kortus, I.I. Mazin, K.D. Belashchenko, V.P. Antropov, and L.L. Boyer, Phys. Rev. Lett. **86**, 4656 (2001).

[61] J.M. An and W.E. Pickett, Phys. Rev. Lett. **86**, 4366 (2001).

[62] Y. Kong, O.V. Dolgov, O. Jepsen, and O.K. Andersen, Phys. Rev. B **64**, 020501 (2001).

[63] P.M. Rafailov, M. Dworzak, and C. Thomsen, Solid State Commun. **122**, 455 (2002).

[64] A.M. Prokhorov, N.P. Lyakishev, G.S. Burkhanov, and V.A. Dement'ev, Engl. Neo. Transl. Izv. Akad. Mater. Nauk SSSR, **32**, 1365 (1996) [Inorg. Mater. (Transl. of Neorg. Mater.) **32**, 1195 (1996)].

[65] The electronic bandstructure and density of states were calculated using the full-potential linearized augmented-plane-wave method as implemented in the WIEN97 code (Ref. 66). For the exchange-correlation potential, we employed the generalized gradient approximation of Ref. 67. Scalar-relativistic corrections were included. The Al $2p$ states were treated as band states using the local orbital extension of the LAPW method (Refs. 66, 68) For k-point sampling employing the tetrahedron method, 296 points were used in the irreducible wedge of the Brillouin zone (4536 in total); other parameters were $R_{MT}K_{max} = 8.0$; $R_{MT} = 1.8$ and 1.4 a_B for Al and B, respectively; $l_{max} = 10$; $G_{max} = 15$.

[66] P. Blaha, K. Schwarz, and J. Luitz, *WIEN97, A Full Potential Linearized Augmented Plane Wave Package for Calculating Crystal Properties* (Karlheinz Schwarz, Technische Universität Wien, Austria, 1999).

[67] J.P. Perdew, S. Burke, and M. Ernzerhof, Phys. Rev. Lett. **77**, 3865 (1996).

[68] D. Singh, Phys. Rev. B **43**, 6388 (1991).

[69] M.V. Indenbom, L.S. Uspenskaya, M.P. Kulakov, I.K. Bdikin, and S.A. Zverkov, Pis'ma v Zhurnal ksperimental'noĭ i Teoreticheskoĭ Fiziki **74**, 304 (2001) [JETP Lett. **74**, 274 (2001)].

[70] L. Boeri, G.B. Bachelet, E. Cappelluti, and L. Pietronero, Phys. Rev. B **65**, 214501 (2002).

[71] B. Renker, K.B. Bohnen, R. Heid, D. Ernst, H. Schober, M. Koza, P. Adelmann, P. Schweiss, and T. Wolf, Phys. Rev. Lett. **88**, 067001 (2002).

[72] M.E. Jones and R.E. Marsh, J. Am. Chem. Soc. **76**, 1434 (1954).